Structure of Mammalian Cytochrome P450 2C5 Complexed with Diclofenac at 2.1 Å Resolution: Evidence for an Induced Fit Model of Substrate Binding[†,‡]

Michael R. Wester,[§] Eric F. Johnson,*[,§] Cristina Marques-Soares,[||] Sylvie Dijols,[||] Patrick M. Dansette,[||] Daniel Mansuy,[||] and C. David Stout*[,⊥]

Department of Molecular and Experimental Medicine, The Scripps Research Institute, 10550 North Torrey Pines Road, MEM-255, La Jolla, California 92037, Laboratoire de Chimie et Biochimie Pharmacologiques et Toxicologiques, UMR 8601 CNRS, Université Paris V, 45, Rue des Saints-Pères, 75270 Paris Cedex 06, France, and Department of Molecular Biology, The Scripps Research Institute, 10550 North Torrey Pines Road, MB8, La Jolla, California 92037

Received April 7, 2003; Revised Manuscript Received June 2, 2003

ABSTRACT: The structure of the anti-inflammatory drug diclofenac bound in the active site of rabbit microsomal cytochrome P450 2C5/3LVdH was determined by X-ray crystallography to 2.1 Å resolution. P450 2C5/3LVdH and the related enzyme 2C5dH catalyze the 4′-hydroxylation of diclofenac with apparent K_m values of 80 and 57 μM and k_{cat} values of 13 and 16 min^{-1}, respectively. Spectrally determined binding constants are similar to the K_m values. The structure indicates that the π-electron system of the dichlorophenyl moiety faces the heme Fe with the 3′- and 4′-carbons located 4.4 and 4.7 Å, respectively, from the Fe. The carboxyl moiety of the substrate is hydrogen bonded to a cluster of waters that are also hydrogen bonded to the side chains of N204, K241, S289, and D290 as well as the backbone of the protein. The proximity of the diclofenac carboxylate to the side chain of D290 together with an increased binding affinity at lower pH suggests that diclofenac is protonated when bound to the enzyme. The structure exhibits conformational changes indicative of an adaptive fit to the substrate reflecting both the hydration and size of the substrate. These results indicate how structurally diverse substrates are recognized by drug-metabolizing P450 enzymes.

Drug-metabolizing P450s such as the CYP2C enzymes generally catalyze the oxidation of structurally diverse substrates that differ in size and functionality. In addition, the reactions that are catalyzed are diverse and include the hydroxylation of saturated and unsaturated hydrocarbons as well as heteroatom oxidation. In some cases, the products reflect oxidation at different sites on the substrate molecule. Although each enzyme exhibits a wide-ranging and overlapping substrate selectivity profile, individual P450s can be major determinants for the clearance of specific drugs. The individual human 2C enzymes contribute significantly to the metabolism of specific drugs used in clinical practice, and adverse drug−drug interactions can arise when one drug modulates the metabolism of the other by these enzymes (*1*). In addition, genetic variation in the properties or expression of these enzymes can lead to adverse drug reactions (*2*). The structural features of these enzymes that underlie their catalytic diversity and substrate selectivity are poorly understood.

The crystallization of a modified form of rabbit P450 2C5, 2C5/3LVdH (*3*), makes direct structural characterization of substrate binding possible. P450 2C5 was originally characterized as a progesterone 21-hydroxylase that is polymorphically expressed in rabbit liver (*4*, *5*). The enzyme was engineered for crystallization by modifying the N-terminal sequence to remove a transmembrane domain that consists of a single hydrophobic helix to yield a membrane-associated protein that can be displaced from membranes by a high ionic strength. The truncated enzyme, designated 2C5dH, was also modified to include a four-histidine tag at the C-terminus. The incorporation of five additional amino acid substitutions derived from the related enzyme 2C3 produced a chimeric protein, 2C5/3LVdH, that was crystallized for structure determination (*6*). The first structure was determined at 3.0 Å resolution for the enzyme crystallized in the absence of a substrate [PDB entry 1DT6 (*3*)].

In an effort to establish structure−function relationships that would aid in understanding human drug metabolism by CYP2C enzymes, we began a systematic examination of P450 2C5's capacity to metabolize substrates for the human CYP2C enzymes. These studies identified 4-methyl-*N*-methyl-*N*-(2-phenyl-2*H*-pyrazol-3-yl)benzenesulfonamide (DMZ)[1] (Figure 1) as a common substrate of 2C5 and the human CYP2C enzymes (*7*). The structure of DMZ bound in the active site of 2C5/3LVdH was determined at 2.3 Å resolution (*8*). DMZ is an analogue of sulfaphenazole, a

[†] This investigation was supported by NIH Grants GM31001 (E.F.J.) and GM59229 (C.D.S.) and by CNRS and the French Minister of Research (D.M.). C.M.-S. was a recipient of a CNRS-Aventis fellowship.

[‡] Structural coordinates have been deposited with the Protein Data Bank as entry 1NR6.

* To whom correspondence should be addressed: Department of Molecular Biology, The Scripps Research Institute, 10550 N. Torrey Pines Rd., MB8, La Jolla, CA 92037. E-mail: dave@scripps.edu. Phone: (858) 784-8738. Fax: (858) 784-2857.

[§] Department of Molecular and Experimental Medicine, The Scripps Research Institute.

[||] Université Paris V.

[⊥] Department of Molecular Biology, The Scripps Research Institute.

10.1021/bi034556l CCC: $25.00
Published on Web 07/19/2003

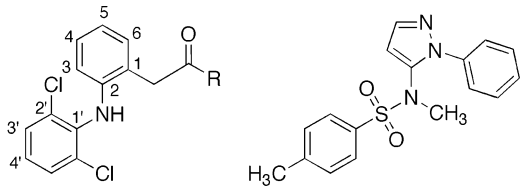

Diclofenac R = OH **DMZ**

Diclofenac amide R = NH2

FIGURE 1: Formulas of diclofenac, diclofenac amide, and DMZ.

selective inhibitor of human P450 2C9, in which the sulfonamide nitrogen is methylated and a methyl group replaces the *p*-amino group on the phenyl ring. P450 2C5 predominantly catalyzes the hydroxylation of the benzylic methyl group of DMZ, as do all four human CYP2C enzymes (*7*). A comparison of the structure of the DMZ complex to the enzyme crystallized in the absence of substrate indicated a significant change in the conformation of the protein around the active site when DMZ binds (*8*).

As the observed conformation changes might depend on the structure of the substrate, we have also determined the structure of the enzyme with diclofenac bound in the active site. Diclofenac (Figure 1) is hydroxylated in a highly regioselective manner, at position 4′, by human CYP2C9, whereas the other human CYP2C enzymes, 2C8, 2C18, and 2C19, produce mixtures of 4′- and 5-hydroxydiclofenac (*9*). These studies identified diclofenac as a substrate for 2C5 that is 4′-hydroxylated with a relatively high catalytic efficiency and that exhibits the same regioselectivity of metabolism as 2C9. Diclofenac is significantly smaller than DMZ (Figure 1) and exhibits a distinct shape that does not overlay the conformation of DMZ when bound to the enzyme. In contrast to the largely hydrophobic DMZ substrate, diclofenac is an anion at neutral pH.

The structural characterization of the CYP2C5−diclofenac complex was undertaken to understand how the carboxyl moiety of the substrate contributes to binding of the substrate as well as potential differences in the conformation of the enzyme that might arise from the different size, polarity, and stereochemical features of the substrate. This is also the first structural characterization of a substrate bound in the active site of the enzyme that undergoes an aromatic hydroxylation. The substrate is positioned so that the π-electron system of the 3′−4′ bond is adjacent to the binding site of the reactive oxygen intermediate. The diclofenac carboxyl group is hydrogen bonded to a network of waters that remain in the distal portion of the active site that is not filled by the substrate. The structure reveals significant changes in the conformation of the protein that are similar but distinct when compared to those induced by the binding of DMZ. The differences in the protein conformations of the DMZ and diclofenac complexes reflect changes to accommodate the hydration of the polar moiety and differences in the volume occupied by diclofenac relative to DMZ. This conformational flexibility is likely to contribute to the capacity of the CYP2C enzymes to metabolize diverse substrates. In addition, the residual hydration of the distal portion of the active site provides a flexible and efficient means of hydrating polar moieties of structurally diverse substrates.

EXPERIMENTAL PROCEDURES

Diclofenac Hydroxylation. CYP2C5dH or CYP2C5/3LVdH (12 pmol) and purified human P450 reductase (0.36 unit) were reconstituted in 50 μL of 50 mM HEPES buffer (pH 7.6) containing 1.5 mM $MgCl_2$ and 0.1 mM EDTA. Following incubation of this mixture for 10 min in ice, the reconstituted enzyme was diluted to 350 μL with the same buffer, containing diclofenac (Sigma), and placed in a shaking bath at 37 °C. The reaction was initiated ($t_0 = 0$ min) by the addition of an NADPH-generating system (1 mM $NADP^+$, 10 mM glucose 6-phosphate, and 2 units of glucose-6-phosphate dehydrogenase/mL). At t_0 and regularly thereafter, aliquots (80 μL) were taken. The reaction was quickly stopped in each aliquot by treatment with 50 μL of a cold CH_3CN/CH_3COOH (10/1) mixture. After centrifugation (10000*g* for 5 min in an Eppendorf centrifuge), the supernatants were analyzed by HPLC using an X-terra MS C18 column (Waters) (250 mm × 4.6 mm, 5 μm). The mobile phases of 25 mM NH_4HCO_3 (pH 7.8) (A) and CH_3CN (B) were delivered at a rate of 1 mL/min with the following gradient: 2 min at 20% B, a 16 min linear gradient to 28% B, then a 3 min linear gradient to 50% B, and a return to 20% B at 25 min. The column effluent was monitored with a scanning Spectra Focus UV detector between 250 and 320 nm. The retention times for 4′-hydroxydiclofenac, 5-hydroxydiclofenac, the internal standard tienilic acid, and the substrate diclofenac were 15, 19, 21, and 24 min, respectively. K_m and k_{cat} were derived from analysis of double-reciprocal plots of the rate of product formation versus the initial substrate concentration using Kaleidagraph 3.0.

Human P450 reductase was isolated following its expression in *Escherichia coli* and purified as described previously (*6*). The activity of the purified reductase preparation was determined spectrophotometrically (*10*). The reductase exhibited a specific activity of 26 units/mg of protein (where a unit is defined as 1 μmol of cytochrome *c* reduced/min). CYP2C5dH and CYP2C5/3LVdH were expressed and purified as described previously (*6*). The average specific contents of the preparations of P450 2C5dH and 2C5/3LVdH were 16.5 and 15.4 nmol/mg of protein, respectively. 4′- and 5-hydroxydiclofenac were gifts from CIBA-GEIGY.

The expression system used for human liver P450s was based on the W(R)fur1 yeast strain, described previously (*11*), in which yeast cytochrome P450 reductase was overexpressed. Transformation by the pYeDP60 vector containing the human liver CYP2C9 cDNA was then performed according to a general construction method of the W(R)fur1 yeast strain expressing various human liver cytochrome P450s (*12*, *13*). Yeast culture and the preparation of microsomes were achieved with techniques described previously (*14*). Microsomes were suspended in a 50 mM Tris buffer (pH 7.4) containing 1 mM EDTA and 20% (v/v) glycerol, aliquoted, frozen under liquid N_2, and stored at −80 °C until they were used. The P450 content of yeast

[1] Abbreviations: CYP, cytochrome P450; DMSO, dimethyl sulfoxide; DFC, diclofenac {2-[(2,6-dichlorophenyl)amino]benzeneacetic acid}; DMZ, 4-methyl-*N*-methyl-*N*-(2-phenyl-2*H*-pyrazol-3-yl)benzenesulfonamide; DTT, dithiothreitol; EDTA, ethylenediaminetetraacetic acid; F_o, observed structure factor; F_c, calculated structure factor; HEPES, *N*-(2-hydroxyethyl)piperazine-*N*′-2-ethanesulfonic acid; PDB, Protein Data Bank; rms, root-mean-square; SSRL, Stanford Synchrotron Radiation Laboratory.

microsomes was 90 pmol of P450/mg of protein. The microsomal P450 content was determined according to the method of Omura and Sato (*15*). The protein content was determined by the Lowry procedure using bovine serum albumin as a standard (*16*).

Determination of the Extent of Substrate Binding to CYP2C5dH, CYP2C5/3LVdH, or CYP2C9 by Difference Visible Spectroscopy. Difference, visible spectra were recorded at room temperature. Purified CYP2C5dH or CYP2C5/3LVdH was diluted in 50 mM HEPES buffer (pH 7.6) containing 1.5 mM $MgCl_2$ and 0.1 mM EDTA, to obtain a P450 concentration of 0.3−0.8 μM. Microsomes from yeast expressing CYP2C9 were suspended in 50 mM Tris buffer (pH 7.4) containing 1 mM EDTA, to obtain a P450 concentration of 0.2 μM. Each solution was divided equally between two quartz cuvettes (1 cm path length, 150 μL for the purified enzymes and 500 μL for the microsomes), and a baseline was recorded. Aliquots of a solution containing the studied compound in DMSO (0.2−1 μL) were added to the sample cuvette, and the same volume of solvent was added to the reference cuvette. The difference spectra were recorded between 380 and 520 nm. UV−visible spectra were recorded on an Aminco DW-2 spectrophotometer modified by Olis Inc.

Synthesis of 2-[2-(2,6-Dichlorophenyl)amino]phenyl Acetamide (Diclofenac Amide). 1,3-Dicyclohexylcarbodiimide (510 mg, 2.47 mmol) was added to a solution of diclofenac (sodium salt, 635 mg, 2 mmol), *N*-hydroxysuccinimide (230 mg, 2 mmol), and ammonium chloride (120 mg, 2.2 mmol), in cold, anhydrous dioxane (6 mL) at 12 °C. The mixture was stirred at room temperature for 24 h. The solid product was filtered and washed with ethyl acetate. Following the evaporation of the solvent, the activated ester was dissolved in dioxane (1 mL) and NH_3-saturated dioxane (5 mL) was added. The completeness of the reaction was monitored by thin-layer chromatography [SiO_2, cyclohexane/ethyl acetate (7/3)]. The solution was diluted with water, extracted with ethyl acetate, and dried over $MgSO_4$. The product was purified by column chromatography [SiO_2, cyclohexane/ethyl acetate (7/3)]. Two recrystallizations from a cyclohexane/ethyl acetate mixture (7/3) gave diclofenac amide in a 20% yield: mp 190 °C [lit. (*17*) 188−189 °C]; ^{1}H NMR ($CDCl_3$) δ 7.33 (d, 2H, $J = 7.8$), 7.19−7.08 (m, 3H), 7.01−6.88 (m, 2H), 6.51 (d, 1H, $J = 7.6$), 5.72 and 5.39 (2 bs, NH_2), 3.70 (s, 2H). Chemical shifts are reported downfield from $(CH_3)_4$-Si, and coupling constants are in hertz. The abbreviations s, bs, d, and m are used for singlet, broad singlet, doublet, and multiplet, respectively. ^{1}H NMR spectra were recorded at 27 °C on a Bruker ARX-250 instrument.

Structure Determination. P450 2C5/3LVdH was purified in high-salt buffers without the use of detergents, as described previously (*18*). Briefly, *E. coli*-expressed 2C5/3LVdH was harvested from 3.0 L of culture by centrifugation, lysozyme treatment, and sonication. The P450 was purified by metal ion affinity column chromatography followed by hydroxylapatite chromatography. The purified protein was concentrated and the buffer exchanged for 50 mM potassium phosphate buffer (pH 7.4) containing 500 mM NaCl, 1 mM EDTA, 0.2 mM DTT, and 20% glycerol using a centrifugal concentrating device. Sodium diclofenac was obtained from Sigma, prepared as a concentrated aqueous solution, and combined with an equimolar amount of the protein. The complex was crystallized with the vapor diffusion method using 2.5 μL hanging drops containing 0.24 mM P450, 0.24 mM diclofenac, 2.4 mM CYMAL-5 detergent (Anatrace), 1.1 M ammonium sulfate, 0.05 M HEPES (pH 7.8), 0.5% PEG400, 20 mM potassium phosphate (pH 7.4), 200 mM NaCl, 0.4 mM EDTA, 0.08 mM DTT, and 8% glycerol. The drops were equilibrated against 2.2 M ammonium sulfate containing 0.1 M HEPES (pH 7.8) and 1% PEG400 at 24 °C. The crystal was prepared for data collection by briefly soaking it in 2.2 M ammonium sulfate containing 0.1 M HEPES (pH 7.8), 1% PEG400, and 20% sucrose as a cryoprotectant followed by flash freezing in liquid N_2 (*18*) and transfer to the cryogenic stream maintained at 100 K. Data were collected at Stanford Synchrotron Radiation Laboratory (SSRL) beam line 11-1 from a single crystal with dimensions of 0.3 mm × 0.3 mm × 0.3 mm. The data were processed with CCP4 programs Mosflm and Scala (*19*, *20*), and a statistical analysis of the X-ray diffraction data is presented in Table 1.

Table 1: Data Collection and Refinement Statistics

	CYP2C5/3LVdH
no. of crystals	1
complex	diclofenac
space group	*I*222
unit cell dimensions (*a*, *b*, *c*) (Å)	73.95, 130.03, 172.78
Data Collection	
SSRL beam line	11-1
wavelength (Å)	0.965
resolution range (Å)	50.0−2.10
total no. of observations	185186
no. of unique reflections of $>0.0\sigma_F$	48402
redundancy[a]	3.8 (2.8)
completeness (%)[a]	99.1 (98.5)
$\langle I/\sigma_I \rangle$[a]	13.4 (1.7)
$R_{symm}(I)$[a]	0.072 (0.565)
Refinement	
R-factor	0.231
R_{free} (5% of data)	0.268
rms deviation for bonds (Å)	0.008
rms deviation for angles (deg)[b]	1.34

Model	no. of atoms	avg *B*-factor (Å^2)
protein[c]	3698	46.2
heme	43	29.3
diclofenac	19	65.6
water molecules	262	51.7
sulfate ions	10	62.9

[a] Values for the highest-resolution shell in parentheses. $\langle I/\sigma_I \rangle$ values of <2.0 are accepted because there is some anisotropy in the diffraction. [b] Ramachandran plot: 86.9% of residues in most favored regions, 10.8% in allowed regions, 1.2% in generously allowed regions, and 1.1% in disfavored regions. [c] Residues 27−488 of the CYP2C5/3LVdH construct.

The complex crystallized in the same space group, *I*222, as crystals used to determine the structures of the DMZ complex and of the enzyme crystallized in the absence of a substrate. However, the unit cell dimensions were different. The original structure of P450 2C5/3LVdH (PDB entry 1DT6) served as the preliminary model for a molecular replacement solution. Rigid body refinement at 4.0, 3.5, and subsequently 3.0 Å resolution was used for the initial refinement. Standard refinement protocols against the 2.1 Å data were employed using CNS (*21*). The program Xfit/Xtalview (*22*) was used for the interpretation, editing, and adjustment of the model into unbiased σ_A-weighted $2|F_o| -$

Table 2: Comparison of the Kinetic Constants of the Hydroxylation of Diclofenac by CYP2C5dH and 2C5/3LVdH with Those of Human CYP2Cs[a]

product		CYP2C5dH	2C5/3LVdH	2C8	2C9	2C18	2C19
4′-OH	k_{cat} (min^{-1})	16 ± 1	13 ± 1	1.2 ± 0.2	24 ± 1	1.1 ± 0.2	1.4 ± 0.5
	K_m (μM)	57 ± 8	80 ± 10	630 ± 30	15 ± 8	170 ± 30	440 ± 50
	k_{cat}/K_m ($min^{-1}\,\mu M^{-1}$)	0.28	0.16	0.002	1.6	0.006	0.003
5-OH	k_{cat} (min^{-1})	traces[b]	traces[b]	7 ± 1	nd[c]	3 ± 0.4	1.1 ± 0.5
	K_m (μM)			280 ± 30	280 ± 30	125 ± 20	470 ± 50
	k_{cat}/K_m ($min^{-1}\,\mu M^{-1}$)			0.02	0.02	0.02	0.002

[a] Conditions used for CYP2C5 and 2C5/3LVdH are described in Experimental Procedures. Mean values ± the standard deviation from three to five experiments. Data indicated for human CYP2Cs were published previously (*9*). [b] Only traces of 5-hydroxydiclofenac were detected by HPLC; this did not allow us to make any quantitative measurements. [c] Formation of 5-hydroxydiclofenac was under our detection limit.

$|F_c|$ composite omit and $|F_o| - |F_c|$ electron density maps. Model building and refinement proceeded through multiple rounds in concert with interpretation and refinement of the structure of the DMZ complex at 2.3 Å resolution (*8*). The model has good main chain and side chain stereochemistry with only eight residues in generously allowed or disallowed regions of the Ramachandran plot (Table 1). Coordinates for the diclofenac complex of P450 2C5/3LVdH have been deposited in the Protein Data Bank as entry 1NR6.

RESULTS

Oxidation of Diclofenac Catalyzed by CYP2C5dH and CYP2C5/3LVdH. Aerobic incubation of diclofenac with recombinant, purified CYP2C5/3LVdH, in the presence of purified human liver cytochrome P450 reductase and an NADPH-generating system, at pH 7.6, led to the almost exclusive formation of 4′-hydroxydiclofenac (Table 2). Only traces of 5-hydroxydiclofenac were formed under those conditions. CYP2C5dH exhibited an identical behavior. The dependence of the rate on the initial substrate concentration for the 4′-hydroxylation of diclofenac catalyzed by CYP2C5dH and CYP2C5/3LVdH exhibited a classical hyperbolic behavior, leading to similar k_{cat} (16 ± 1 and 13 ± 1 min^{-1}, respectively) and K_m values (57 ± 8 and 80 ± 10 μM, respectively) (Table 2). When compared to the human CYP2Cs, CYP2C5dH and CYP2C5/3LVdH exhibited a regiospecificity similar to that of CYP2C9, as these enzymes almost exclusively produce 4′-hydroxydiclofenac, whereas CYP2C8, 2C18, and 2C19 yield mixtures of 4′-hydroxy- and 5-hydroxydiclofenac (Table 2). The k_{cat} and K_m values of 4′-hydroxylation of diclofenac by the two 2C5 proteins were intermediate between those previously described for CYP2C9 and for the other human CYP2Cs. However, the catalytic efficiency is much closer to that found for CYP2C9 (Table 2).

Characterization of Diclofenac Binding to CYP2C5 Proteins by Visible Difference Spectroscopy. CYP2C5dH and 2C5/3LVdH exhibit visible spectra that are typical of predominantly low-spin Fe(III) P450 enzymes, in 50 mM HEPES buffer (pH 7.6), with a Soret peak at 417 nm (data not shown). Addition of diclofenac led, in both cases, to the appearance of a type I difference spectrum characterized by a peak at 395 nm and a trough at 420 nm that corresponds to an increased population of the high-spin state of the heme protein (*23*).

The plot of $1/\Delta A$ (395−420 nm) versus 1/[diclofenac] obtained from spectral titration of CYP2C5dH with diclofenac revealed an estimated binding constant of 58 ± 10 μM. A second low-affinity component was apparent at concentrations of diclofenac that exceeded 100 μM with an estimated binding constant of 295 ± 30 μM. Almost identical results were found in the case of CYP2C5/3LVdH, with apparent K_s values of 55 ± 10 and 280 ± 40 μM (Table 3). It is noteworthy that the high-affinity K_s values correspond closely to the K_m values calculated for 4′-hydroxylation of diclofenac (K_{s1} = 58 ± 10 and K_m = 57 ± 8 μM for CYP2C5dH; K_{s1} = 55 ± 10 and K_m = 80 ± 10 μM for CYP2C5/3LVdH). This result suggests that the high-affinity binding site for this drug is involved in the 4′-hydroxylation of diclofenac.

Table 3: Dissociation Constants for the Complexes of Diclofenac and Diclofenac Amide with CYP2C5dH, 2C5/3LVdH, and CYP2C9 Measured by Difference Visible Spectroscopy[a]

	K_s (μM)		
	CYP2C5dH	CYP2C5/3LVdH	CYP2C9
diclofenac	K_{s1} = 58 ± 10	55 ± 10	16 ± 2
	K_{s2} = 295 ± 30	280 ± 40	
diclofenac amide	12 ± 1	11 ± 1	110 ± 10

[a] Conditions in Experimental Procedures. Mean values ± the standard deviation from four experiments.

Titration of recombinant CYP2C9 with diclofenac also led to a type I difference spectrum, and to a single K_s value of 16 ± 2 μM, which is 4-fold lower than those determined for the CYP2C5 proteins (Table 3). Similar spectral titrations were also performed with the amide of diclofenac (Figure 1). In contrast to diclofenac, which mainly exists as an anion at pH 7.6, the neutral amide derivative of diclofenac produced reverse type I difference spectra characterized by a peak at 419 nm and a trough at 395 nm when added to CYP 2C9, 2C5dH, and 2C5/3LVdH. The formation of the CYP2C−diclofenac amide complexes were characterized by K_s values that were much lower for the CYP2C5 proteins than for CYP2C9 (12 and 11 ± 1 μM vs 110 ± 10 μM, respectively; Table 3). These results suggested that the neutral form of diclofenac is likely to bind to the CYP2C5 proteins more favorably than the anion, whereas CYP2C9, which seems to prefer anionic compounds, readily binds the anionic form of diclofenac as previously reported (*24*). To confirm this possibility, the effects of pH on the interaction of diclofenac with CYP2C5dH and 2C5/3LVdH were examined.

Effects of pH on the Interaction between Diclofenac and CYP2C5dH and 2C5/3LVdH. Table 4 shows that decreasing the pH from 7.6 to 5.3 led to a progressive decrease of the K_{s1} value deduced from spectral titration of CYP2C5/3LVdH with diclofenac (from 55 ± 10 to 12 ± 1 μM). Here too, CYP2C5dH exhibited a behavior almost identical to that of CYP2C5/3LVdH (Table 4). Decreasing the pH from 7.6 to 5.3 led not only to a clear increase in the affinity of

Table 4: Effect of pH on the Interaction of CYP2C5dH and 2C5/3LVdH with Diclofenac Determined by Difference Visible Spectroscopy[a]

	2C5/3LVdH			2C5dH	
	pH 5.3	pH 6.5	pH 7.6	pH 5.3	pH 7.6
K_{s1} (μM)	12 ± 1	30 ± 3	55 ± 10	11 ± 1	58 ± 10
K_{s2} (μM)	50 ± 5	200 ± 30	280 ± 40	45 ± 5	295 ± 30
% spin state change[b]	75	60	25	70	50

[a] Conditions in Experimental Procedures. Mean values ± the standard deviation from four experiments. [b] Percentage spin state change calculated from the maximum intensity of the difference spectrum, assuming an $\epsilon_{395-420}$ of 120 mM^{-1} cm^{-1} (*23*).

Table 5: Effect of pH on the Kinetic Constants of the 4′-Hydroxylation of Diclofenac by CYP2C5dH and 2C5/3LVdH[a]

	pH 5.3		pH 7.6	
	2C5dH	2C5/3LVdH	2C5dH	2C5/3LVdH
k_{cat} (min^{-1})	5.5 ± 1	1.4 ± 0.6	16 ± 1	13 ± 1
K_m (μM)	20 ± 5	21 ± 5	57 ± 8	80 ± 10
k_{cat}/K_m (min^{-1} μM^{-1})	0.27	0.07	0.28	0.16

[a] Conditions in Experimental Procedures. Mean values ± the standard deviation from three to five experiments. At pH 7.6, only traces of 5-hydroxydiclofenac could be detected, whereas quantitation of this metabolite was possible at pH 5.3 (k_{cat} = 0.7 and 0.2 min^{-1} for CYP2C5dH and CYP2C5/3LVdH, respectively).

diclofenac for CYP2C5/3LVdH, but also to a dramatic increase in the intensity of the spin state change of this heme protein. In fact, the maximum intensity of the difference spectrum observed at pH 7.6 corresponded to ~25% conversion of the heme protein from the low-spin to the high-spin state, whereas at pH 5.3, the conversion corresponds to 75% of CYP2C5/3LVdH (Table 4).

The effects of pH on the kinetic constants of CYP2C5dH- and 2C5/3LVdH-catalyzed 4′-hydroxylation of diclofenac were also studied. The results indicate that the reconstituted monooxygenase system consisting of purified CYP2C5dH (or 2C5/3LVdH) and human P450 reductase was sufficiently stable at pH 5.3 to catalyze the 4′-hydroxylation of diclofenac by NADPH and O_2. Table 5 shows that the k_{cat} values found for both CYP2C5 proteins were decreased when the pH was decreased from 7.6 to 5.3. However, the resulting k_{cat}/K_m values were similar because the K_m values calculated for the hydroxylation catalyzed by the two CYP2C5 proteins were also clearly decreased when the pH was decreased, and reached an almost identical value of 20 ± 5 μM at pH 5.3.

This parallel decrease of the K_s value of the CYP2C5−diclofenac complex and of the K_m value for CYP2C5-catalyzed 4′-hydroxylation of diclofenac, when the pH was decreased, confirmed that the CYP2C5 proteins better recognize the neutral (COOH) form of diclofenac. In that regard, it is noteworthy that the K_{s1} and K_m values calculated for the interaction of diclofenac with CYP2C5 proteins at pH 5.3 (~12 and ~20 μM) (Tables 4 and 5) are similar to the K_s values found for diclofenac amide at pH 7.6 (Table 3). In contrast, this change in pH did not alter the apparent K_m for DMZ hydroxylation (not shown). Taken together, these results suggest that the neutral form of diclofenac binds to CYP2C5dH and CYP2C5/3LVdH.

Determination of the Structure of 2C5/3LVdH with Diclofenac Bound in the Active Site. The complex of diclofenac with 2C5/3LVdH was crystallized from solutions of the enzyme and substrate that initially contained each at 0.24 mM. Data collected for a crystal that diffracted to 2.1 Å resolution were used for structure determination. The initial phases were determined by molecular replacement using the original structure determined for the enzyme (PDB entry 1DT6). The complex crystallized in the same space group as crystals used for the original structure and the DMZ complex. However, the unit cell dimensions differed. Significant remodeling of the flexible portions of the active site was required because of changes that occur as a result of substrate binding. The final model exhibits a crystallographic R value of 0.23 and an R_{free} value of 0.27 (Table 1).

The location of diclofenac in the active site was clearly defined by electron density that revealed the presence of the expected, staggered conformation of the two aromatic rings. The aromatic ring distal from the heme iron exhibited Y-shaped density for the carboxyl side chain of the substrate, whereas the aromatic ring closest to the heme Fe exhibited density for the two chlorines (Figure 2a). The location of the dichlorophenyl ring of diclofenac places the 3′- and 4′-carbons closest to the heme Fe at 4.4 and 4.7 Å, respectively. The planar surface of the aromatic ring is oriented toward the iron so that the π-electron system is positioned near the location where reduced oxygen intermediates are bound to the iron during the reaction. This geometry is most consistent with a consensus mechanism for aromatic hydroxylation involving the direct insertion of the oxygen to form an intermediate epoxide that rearranges to yield the 4′-hydroxylated product (*25*, *26*).

Additional density near the carboxyl moiety (Figure 2a) reflects the presence of water molecules that are likely to form an extensive network of hydrogen bonds (Figure 2b). This hydrogen bonding network is anchored to the polar side chains of N204, K241, S289, and D290. The side chain of N204 is also hydrogen bonded to N236; the side chain of K241 is also hydrogen bonded to the backbone carbonyl of V106, and the side chain of D290 is also hydrogen bonded to the backbone amides of I112 and A113 where another water molecule is also bound. This cluster of waters also hydrogen bonds to the peptide backbone of residues A237 and S289. A single water molecule resides on the opposite side of the carboxyl moiety of diclofenac that potentially hydrogen bonds to the amine of diclofenac and the backbone carbonyl of D290. As a result of these hydrogen bonding interactions, the polar moiety of the substrate can be readily accommodated in the active site. This extensive hydration is not evident in the structure of the DMZ complex because the substrate occupies a larger portion of this region (*8*).

Hydration that is more extensive than the evident hydration for the DMZ complex (PDB entry 1N6B) is also seen on the opposite side of the substrate in a cleft on the surface of the enzyme formed by the F helix and β-sheet 4 (Figure 3a). The hydrogen bonding patterns are depicted in Figure 3b along with an ordered water molecule in the characteristic gap in the I helix adjacent to the site of oxygen binding that is generally seen in P450s. The chain of water is anchored to E297 and R304 on helix I and makes extensive interactions with the backbone and side chains of helix F and β-sheet 4. The more extensive hydration of this cleft in the CYP2C5−diclofenac complex reflects a gap between the F helix and β-sheet 4 that is larger than that seen in the complex with

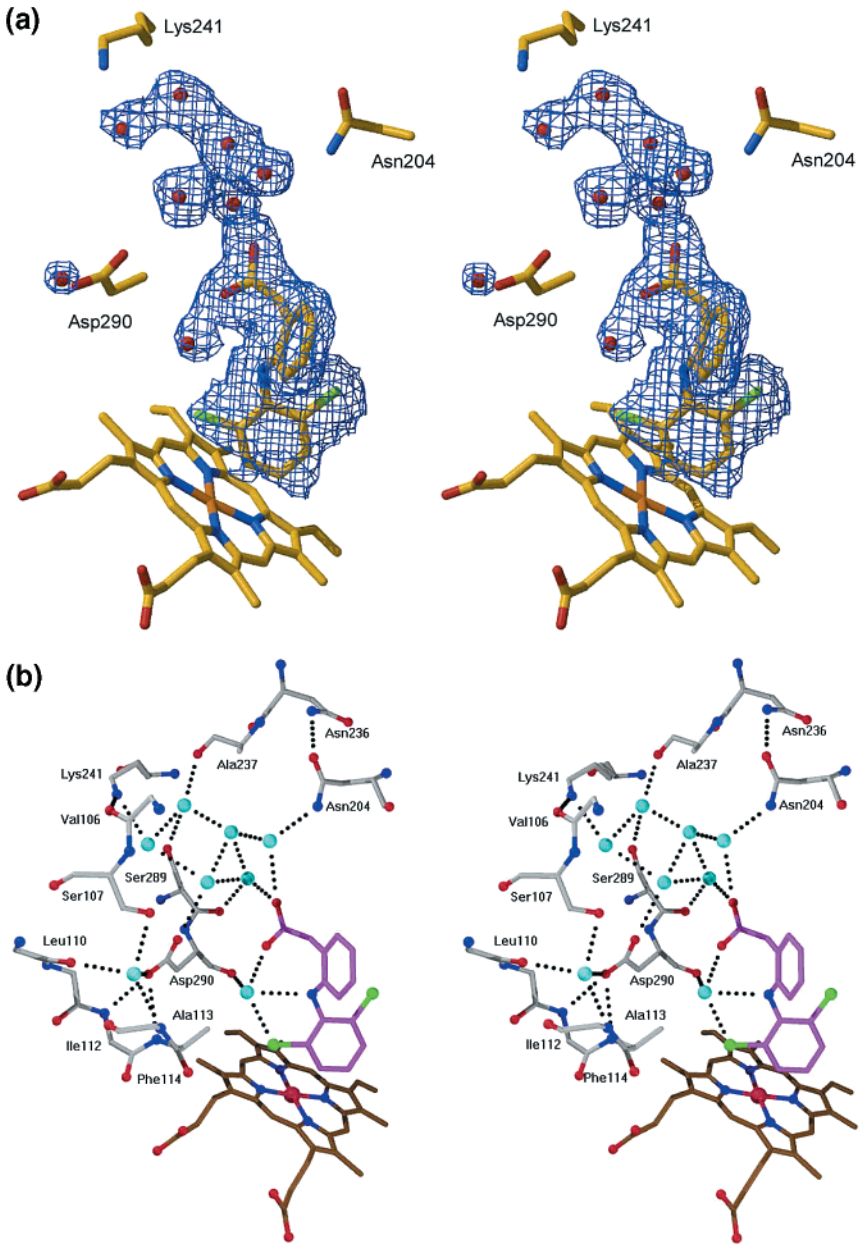

FIGURE 2: (a) Stereoview of the electron density for diclofenac and bound H_2O molecules in the structure of P450 2C5/3LVdH at 2.1 Å resolution. The map is calculated from the model with the substrate and H_2O molecules omitted using σ_A-weighted $2|F_o| - |F_c|$ coefficients and is contoured at 1σ. The substrate, heme, and side chains are rendered as sticks. Waters are rendered as spheres. Atoms are colored yellow for C, blue for N, red for O, green for Cl, and orange for Fe. (b) Stereoview depicting potential hydrogen bonds (dotted black lines) involving diclofenac, bound H_2O molecules, and surrounding residues of helix F (N204), helix G (N236, A237, and K241), helix I (S289 and D290), and the B−C loop (V106, S107, L110, I112, A113, and F114). The view is the same as in panel a. Waters are depicted as cyan spheres. Atoms are colored gray for C, blue for N, red for O and Fe, green for Cl, brown for heme C, and purple for diclofenac C.

DMZ. This reflects conformation changes of flexible elements that form the active site to adapt to the binding of the substrate.

Portions of the superimposed structures for the diclofenac and DMZ complexes are depicted in Figure 4. Overall, the structures are highly superimposable with an rms of 0.66 Å for all 462 Cα atoms. However, flexible portions of the active site adapt to each substrate. Residues in the B−C loop, which display the largest differences between the two structures, are well-defined in the electron density (Figure 4a). The portions of the superimposed Cα traces of the peptide backbones of the diclofenac complex (blue) and DMZ complex (green) are shown in Figure 4b. The largest differences are seen for the region around the B′ helix, residues 100−107, that reflect the smaller size of diclofenac compared to DMZ, and the more extensive hydration in the distal portion of the cavity (Figure 4c). Differences in the locations of the F and G helices are also evident, whereas differences are insignificant for the heme and helix I. In contrast to DMZ, diclofenac occupies a larger volume close to the heme Fe, resulting in a shift of helix F (Figure 4b) as well as a change in the orientation of F473 on the turn in β-sheet 4 (Figure 4c). The resulting cleft between the F helix and β-sheet 4 leads to the increased level of hydration depicted in Figure 3.

The side chain positions of residues that directly contact diclofenac are compared to their positions in the DMZ complex in Figure 4c. The difference in the position of F473

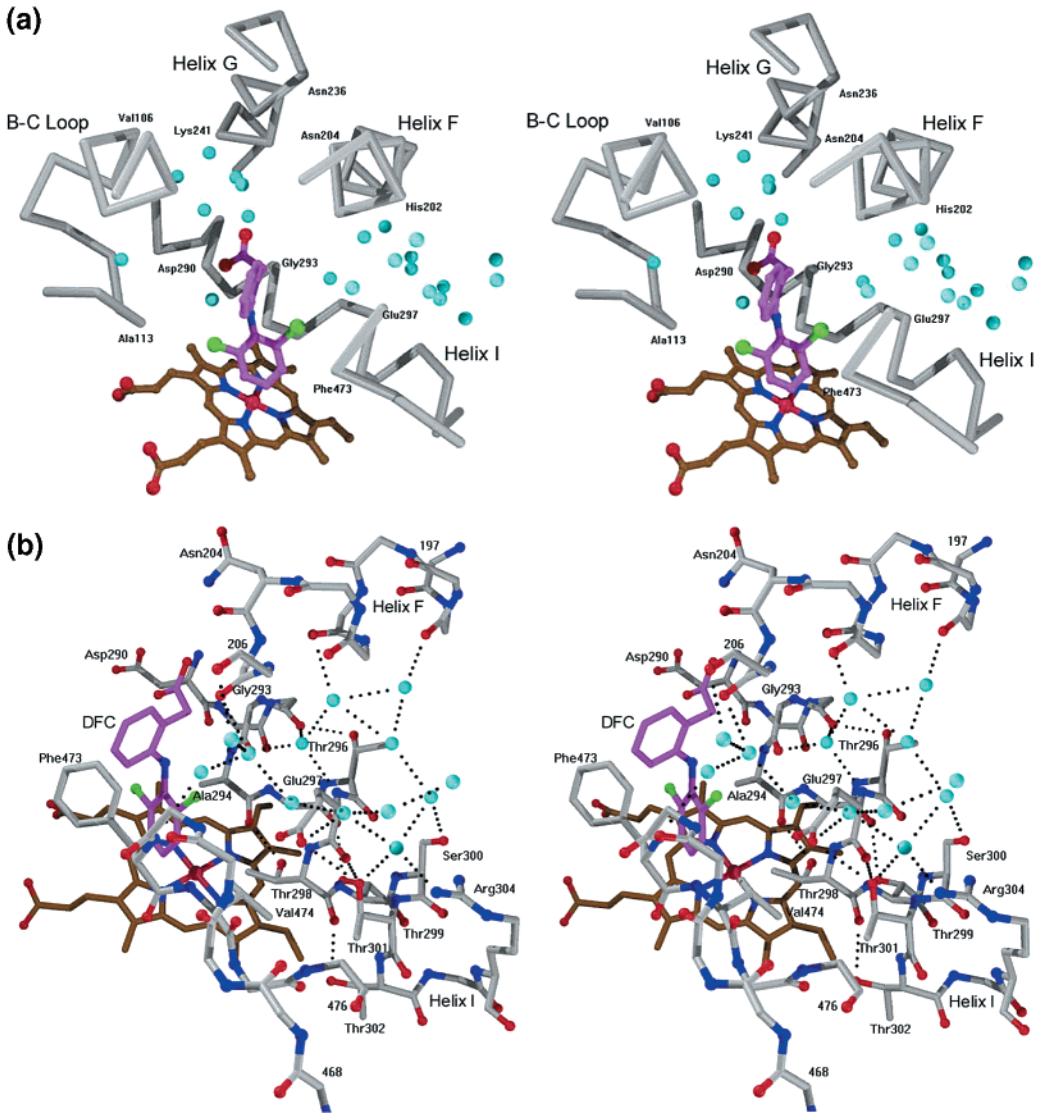

FIGURE 3: (a) Stereoview showing two clusters of bound H_2O molecules in the structure of the diclofenac complex of P450 2C5/3LVdH. One H_2O cluster is associated with diclofenac and Asp290 as depicted in Figure 2. The other H_2O cluster lies in a cleft formed by helices F and I, and the β-loop (β4) containing Phe473, and is associated with E297 and R304, shown in panel b. The two clusters are separated from each other by the substrate. Elements of the protein structure defining the active site are shown as gray tubes linking Cα atoms. H_2O molecules are depicted as cyan spheres. Diclofenac and heme C atoms are purple and brown, respectively, and N, O, and Cl atoms are blue, red, and green, respectively. (b) Stereoview depicting potential hydrogen bonds (dotted black lines) involving H_2O molecules in the cleft formed by helices F and I, and the β4 loop, and associated with E297 and R034. The view is similar to that in panel a. All side chains participating in the hydrogen bonding network are shown, along with side chains on helix I involved in hydrogen bonding. One H_2O molecule is bound within helix I between the carbonyl of G293 and the amide of E297. H_2O molecules and atoms are colored as in panel a.

results in a favorable edge-to-face aromatic interaction with diclofenac. A similar interaction is evident between diclofenac and F114. Mutagenesis experiments with CYP2C9 recently showed that F476 and F114 play an important role in diclofenac recognition (*27*, *28*). It thus appears that $\pi-\pi$ interactions between an aromatic ring of diclofenac and F114 and F473 (F476 in CYP2C9) are important for diclofenac binding to CYP2C5 and CYP2C9. The largest differences in the positions of the contact residues are associated with movements of the backbone described earlier. These are most pronounced for V100 and L103 of the B′ helix, which are shifted by 3.5 and 2.5 Å, respectively, relative to their positions in the DMZ complex. The motion of the B′ helix is hinged at Gly109 at its C-terminal end, allowing the two-turn helix to reorient; the resultant displacement of residues at the N-terminus of this helix is accommodated by main chain torsion angle changes at Gly98 and Ser99. Repositioning of the B′ helix with respect to the GlyXGly98 and Gly109XGly motif residues is consistent with analysis of substrate access in the DMZ complex (Figure 5 in ref *8*).

Mutagenesis experiments with CYP2C9 suggested that either R97 or R108 of CYP2C9 might interact with diclofenac because substitution of alanine at either position greatly diminished the level of diclofenac hydroxylation (*29*). Neither of the corresponding residues (R97 and K108) contacts diclofenac in 2C5/3LVdH. These residues are clearly defined by electron density maps (Figure 4a). R97 is positioned to interact with the propionic acid side chain of the heme, and mutagenesis of this residue might produce

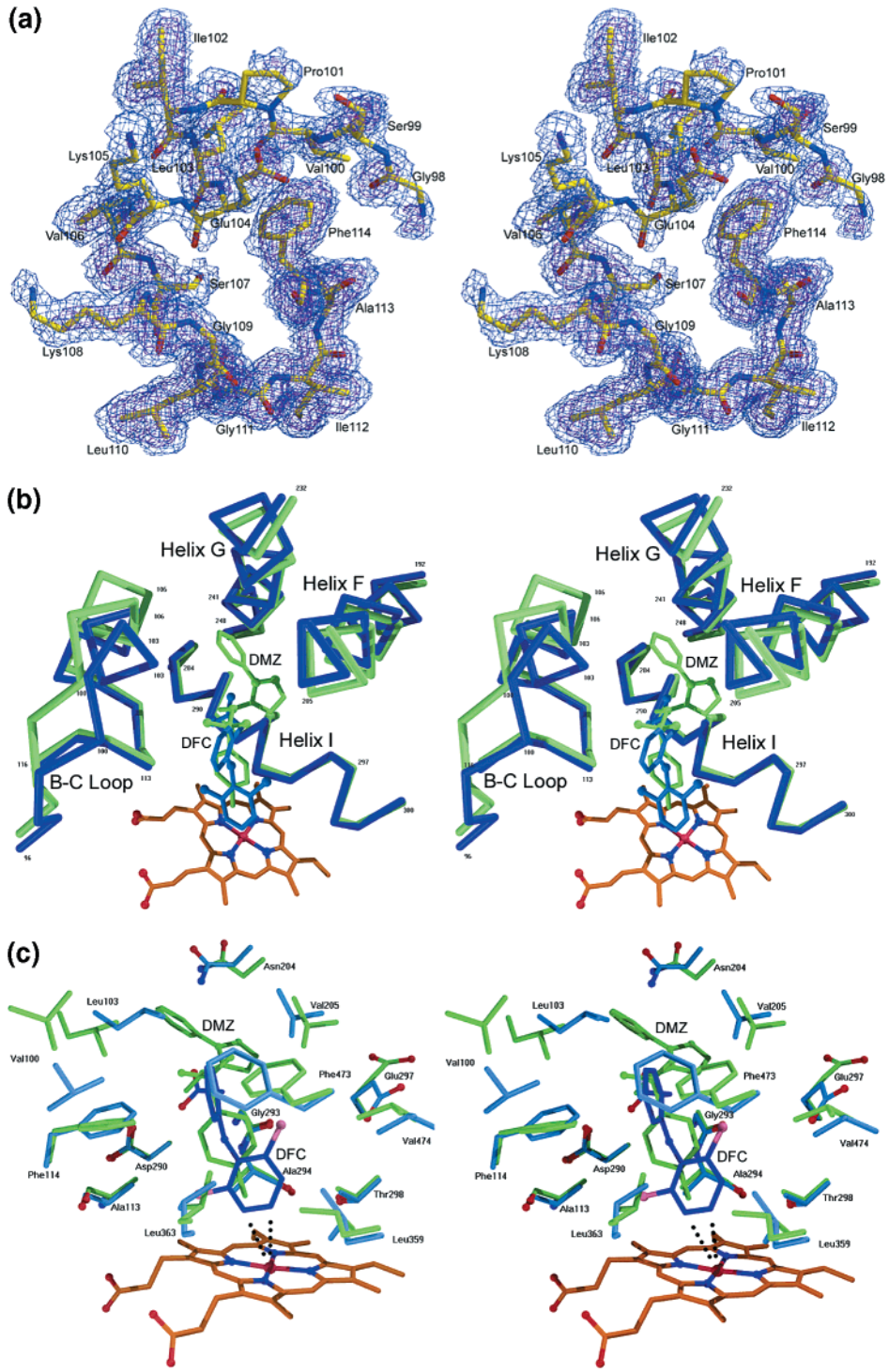

FIGURE 4: (a) Stereoview of the electron density for B−C loop residues 98−114 in the unbiased, composite omit, σ_A-weighted $2|F_o| - |F_c|$ map at 2.1 Å resolution. The map is contoured 1σ and 3σ. (b) Stereoview of the superposition of the structures of the DFC (blue) and DMZ (green) complexes of P450 2C5/3LVdH based on a least-squares fit of all 462 Cα atoms (rmsd of 0.66 Å). (c) Stereoview of the superposition of the structures of the DFC (blue) and DMZ (green) complexes of P450 2C5/3LVdH as in panel b showing the side chains of 15 residues in the DFC complex that are within 5 Å of an atom in diclofenac. For Gly and Ala residues, atoms of the main chain are also shown. The view is similar to that in panel b and highlights how the shift of helical segments results in repositioning of side chains in the active site. Black dotted lines indicate contacts of 4.41 and 4.74 Å between aromatic carbon atoms of diclofenac and the heme Fe. Atoms are colored light blue and green for C, dark blue for DFC C, dark blue for N, red for O, pink for Cl, orange for heme C, and red for Fe.

unintended changes in the structure of the enzyme. K108 is clearly located on the outer surface of 2C5/3LVdH. If R108 of CYP2C9 is involved in forming a salt bridge with diclofenac, the conformation of this region must differ significantly from 2C5. Given the conformational variability of this region in different P450s and its flexibility in 2C5, such conformation differences could contribute to the observed differences in the nature of the diclofenac form that is preferentially bound to CYP2C5 and CYP2C9 proteins (COOH and COO^-, respectively).

DISCUSSION

This study addresses the conformational flexibility of the rabbit equivalent of the human CYP2C drug-metabolizing enzymes and the importance of this flexibility in substrate recognition. The observation that rabbit CYP2C5 regiospecifically hydroxylates the 4′-position of the dichlorophenyl ring of diclofenac prompted us to examine the structure of the enzyme−substrate complex because diclofenac differs in size, conformation, and polarity from DMZ. The presence of chlorine substituents results in a decreased reactivity of the dichlorophenyl ring of diclofenac and disfavors its 4′-hydroxylation. In addition, the anionic carboxyl moiety of the benzeneacetic acid ring is generally expected to promote the solubility of the drug and diminish the affinity for P450s. Human CYP2C9 is distinguished among the principal, human drug-metabolizing P450s by its capacity to selectively catalyze the 4′-hydroxylation of diclofenac with a relatively high catalytic efficiency and affinity for the drug (*9*). This reaction is often used as a reference activity for 2C9, which metabolizes a variety of related nonsteroidal anti-inflammatory drugs. The other drug-metabolizing P450s generally exhibit relatively low catalytic efficiencies and less regioselectivity, hydroxylating both of the aromatic rings of diclofenac.

Ionization of the carboxylate is likely to contribute to the selectivity of specific enzymes for the metabolism of diclofenac by favoring those that can effectively neutralize the substrate by interactions with basic amino acid side chains or by increasing the level of protonation of the substrate at neutral pH. In addition, the relatively specific and stereochemically restricted nature of these interactions contributes to the regiospecificity of metabolism by favoring a single binding orientation. In the case of CYP2C5, diclofenac does not directly interact with a basic residue, but rather, the carboxyl moiety is found in the proximity of the carboxyl of D290. The carboxyl groups of diclofenac and D290 are not directly hydrogen bonded, but they each interact with a cluster of ordered water molecules that are favorably positioned for hydrogen bonding interactions. The disposition of the waters between the two carboxyl groups is unlikely to provide sufficient shielding to weaken the unfavorable electrostatic interactions between negatively charged carboxyl groups at this distance (4.3 Å). This suggests that one or both of these carboxylates are likely to be protonated.

Decreasing the pH to 5.3 increased the binding affinity of CYP2C5 for diclofenac (Tables 4 and 5), suggesting that the neutral form of diclofenac binds to CYP2C5. At pH 5.3, the binding affinity of diclofenac increased 4-fold and was similar to the affinity exhibited by CYP2C5 for the neutral amide of diclofenac at pH 7.6. This pH change did not alter the binding affinity of CYP2C5 for the neutral substrate DMZ (data not shown). This propensity of CYP2C5 to bind neutral compounds better than their anionic analogues has already been reported in the case of sulfaphenazole derivatives (*7*). In contrast, CYP2C9 recognizes anionic compounds (*9*, *24*) such as the anionic form of diclofenac better (ref *24* and Table 3). These results suggest that the interactions between CYP2C5 and CYP2C9 with diclofenac are likely to differ.

The ability of CYP2C5 and CYP2C9 to provide specific interactions with the polar and potentially anionic side chain of diclofenac is likely to facilitate substrate binding and contribute to the high regiospecificity of the hydroxylation exhibited by the two enzymes by favoring a single binding location that accommodates the polar group of the substrate. In the case of CYP2C5, this reflects in part the capacity of the enzyme and substrate to interact with a network of hydrogen-bonded waters that is formed in the unoccupied portion of the substrate binding cavity. Although a variety of such networks might form to facilitate the binding of polar moieties of other substrates, the need to maintain extensive hydrogen bonding interactions for each of the water molecules will be important in creating a favorable free energy of binding. In particular, five of the seven water molecules associated with diclofenac and D290 have their hydrogen bonding capacity fully saturated (Figure 2b). Thus, the capacity to form such ordered networks of water molecules is likely to be an important aspect of substrate specificity in drug-metabolizing enzymes.

Polar side chains, which are relatively rare in the substrate binding cavity, play an important role in the formation of the water cluster seen in the diclofenac complex. In the case of 2C5, D290, S289, K241, and N204 contributed extensively to the stability of the water cluster. It is interesting to note that D290 and N204 are highly conserved in the human 2C subfamily. In contrast, residues that align with S289 and K241 are more varied. This sequence variation coupled with the conformational flexibility of the protein will contribute to differences between enzymes in their capacity to interact with polar substrates.

D290 is also highly conserved within the 2C, 2D, 2E, and 2J subfamilies for all animal species, and this residue has been implicated in the binding of positively charged residues to CYP2D6. Substitution of neutral residues for the conserved aspartate residue of CYP2D6 (*30*, *31*) and CYP2C9 (*32*) generally slows the metabolism of cationic and anionic substrates for each enzyme, respectively. In the case of CYP2D6, neutral substitutions confer a capacity to metabolize diclofenac to the CYP2D6 mutant (*33*). In addition, the neutral substitution did not greatly alter the metabolism of a neutral substrate by CYP2D6 (*34*). D290 is likely to play a key structural role in CYP2C5 as well as the other enzymes because it forms a hydrogen bond to the backbone of the loop between the B′ and C helices. In addition, D290 hydrogen bonds to an ordered water that also hydrogen bonds to S107 of this loop. Thus, amino acid substitutions for D290 are likely to affect both the electrostatic potential experienced by the substrate and the conformation of the B′−C loop and adjacent regions.

In this context, it is interesting to reconsider the potential that the B′−C loop may exhibit a conformation in CYP2C9 that is different from that seen for CYP2C5. An alternate conformation of the loop that would place R108 (K108 in CYP2C5) in the active site would also alter the environment and, possibly, the electrostatic potential seen by the conserved aspartate residue. In contrast, CYP2C19 exhibits a low catalytic efficiency for the hydroxylation of diclofenac. CYP2C9 and CYP2C19 exhibit amino acid sequences that are 90% identical and have identical sequences for the B′−C loop. Studies of chimeric enzymes created between the two enzymes indicate that amino acid differences between the two enzymes adjacent to D290 and the B′−C loop that are outside the substrate binding cavity underlie the selectivity

for mephenytoin (*35*), sulfaphenazole (*36*), and diclofenac (*37*). These observations reinforce the notion that the charge and hydrogen bonding interactions in the vicinity of the conserved aspartate are important determinants of substrate binding affinity and regioselectivity.

The largest conformational difference exhibited by the diclofenac and DMZ complexes is seen for the position of the B′ helix. The N-terminal end of the B′ helix repositions to maximize van der Waals contacts with the two substrates. In addition, changes in the ordered network of waters resulting from the occupancy of the distal portion of the cavity by the larger DMZ molecule are also likely to contribute to the changes seen in the B′−C loop.

The F−G helix region also exhibits significant changes in conformation. These two helices are cantilevered over the top of helix I, which serves as a fulcrum allowing the two helices to rise and fall above the substrate binding cavity to accommodate substrate entry. Two recently described structures for prokaryotic P450s, oxyb (*38*) and CYP154C1 (*39*), exhibit open conformations in the absence of substrate. Helices F and G have pivoted away from the N-terminal β-sheet system in these structures. Substrate-free CYP102 also exhibits an open channel to the active site (*40*). When its fatty acid substrates bind, the carboxyl group of the substrate remains near the entrance to the channel and the remainder of the channel collapses around the hydrocarbon tail. This is accomplished by extensive movements of the F−G region (*41*, *42*). Differences in the conformation of the region between the F and G helices are also seen when the inhibitor-bound (*43*) and substrate-free structures (*44*) of CYP119 are compared.

In the case of CYP2C5, movement of the F−G helices clearly facilitates the binding of structurally diverse substrates. As seen for the DMZ complex, the change in elevation of the F helix above the active site when diclofenac binds is accompanied by movement of helix F across the surface of the helix I perpendicular to the axis of the I helix (*8*). In the case of the diclofenac complex, the pitch of helix F increases relative to the DMZ complex to permit diclofenac to occupy a larger volume near the heme Fe. In contrast, the pitch of the G helix is lowered to maintain its interactions with the B′ helix that has moved in to contact the smaller substrate. As a result, the direction of the axis of helix F changes where it crosses helix I, opening the cleft between helix F and β-sheet 4. As illustrated in Figure 3b, this cleft is extensively hydrated when compared to the DMZ complex. The highly conserved E297 that is thought to be important for proton delivery during catalysis (*45*) anchors this chain of waters together with R304. However, the presence of diclofenac interrupts the continuity between this water channel and the cluster of waters near D290, and effectively isolates the oxygen binding site at the heme iron from these potential proton delivery chains. The binding of diclofenac also positions the dichlorophenyl ring of diclofenac for direct addition of the reduced oxygen intermediate to the π-electron system of the ring to form an intermediate epoxide.

In summary, the structure of the diclofenac complex of CYP2C5/3LVdH provides the first experimental structure of a substrate bound to a P450 enzyme that undergoes aromatic hydroxylation. A comparison of this structure with the DMZ complex of the enzyme (*8*) indicates that significant conformational changes contribute to substrate recognition and binding. The role of ordered networks of water molecules in the binding of the carboxylate moiety of diclofenac suggests an important role for such networks in the binding of polar substrates that occupy only a portion of the substrate binding cavity. The potential to form alternative water networks and the flexibility of the enzyme are likely to underlie the capacity to efficiently metabolize structurally diverse substrates while exhibiting substrate selectivity and regiospecific metabolism.

ACKNOWLEDGMENT

We thank the staff of the Stanford Synchrotron Radiation Laboratory for their generous assistance.

REFERENCES

1. Tanaka, E. (1998) *J. Clin. Pharmacol. Ther. 23*, 403−416.
2. Lee, C. R., Goldstein, J. A., and Pieper, J. A. (2002) *Pharmacogenetics 12*, 251−263.
3. Williams, P. A., Cosme, J., Sridhar, V., Johnson, E. F., and McRee, D. E. (2000) *Mol. Cell 5*, 121−132.
4. Dieter, H. H., Muller-Eberhard, U., and Johnson, E. F. (1982) *Biochem. Biophys. Res. Commun. 105*, 515−520.
5. Dieter, H. H., Muller-Eberhard, U., and Johnson, E. F. (1982) *Science 217*, 741−743.
6. Cosme, J., and Johnson, E. F. (2000) *J. Biol. Chem. 275*, 2545−2553.
7. Marques-Soares, C., Dijols, S., Macherey, A.-C., Wester, M. R., Johnson, E. F., Dansette, P. M., and Mansuy, D. (2003) *Biochemistry 42*, 6363−6369.
8. Wester, M. R., Johnson, E. F., Marques-Soares, C., Dansette, P. M., Mansuy, D., and Stout, C. D. (2003) *Biochemistry 42*, 6370−6379.
9. Mancy, A., Antignac, M., Minoletti, C., Dijols, S., Mouries, V., Duong, N. T., Battioni, P., Dansette, P. M., and Mansuy, D. (1999) *Biochemistry 38*, 14264−14270.
10. Peterson, J. A., and Mock, D. M. (1975) *Anal. Biochem. 68*, 545−553.
11. Truan, G., Cullin, C., Reisdorf, P., Urban, P., and Pompon, D. (1993) *Gene 125*, 49−55.
12. Urban, P., Truan, G., Bellamine, A., Laine, R., Gautier, J. C., and Pompon, D. (1994) *Drug Metab. Drug Interact. 11*, 169−200.
13. Pompon, D., Louerat, B., Bronine, A., and Urban, P. (1996) *Methods Enzymol. 272*, 51−64.
14. Bellamine, A., Gautier, J.-C., Urban, P., and Pompon, D. (1994) *Eur. J. Biochem. 225*, 1005−1013.
15. Omura, T., and Sato, R. (1964) *J. Biol. Chem. 239*, 2379−2385.
16. Lowry, O. H., Rosebrough, N. J., Farr, A. L., and Randall, R. J. (1951) *J. Biol. Chem. 193*, 265−275.
17. Sallmann, A., and Pfister, R. (1969) *Chem. Abstr. 70*, 77619m.
18. Wester, M. R., Stout, C. D., and Johnson, E. F. (2002) *Methods Enzymol. 357*, 73−79.
19. Leslie, A. G. W. (1996) A data collection strategy option in MOSFLM, Collaborative Computational Project No. 4 Newsletter.
20. Collaborative Computational Project No. 4 (1994) *Acta Crystallogr. D50*, 760−763.
21. Brunger, A. T., Adams, P. D., Clore, G. M., DeLano, W. L., Gros, P., Grosse-Kunstleve, R. W., Jiang, J. S., Kuszewski, J., Nilges, M., Pannu, N. S., Read, R. J., Rice, L. M., Simonson, T., and Warren, G. L. (1998) *Acta Crystallogr. D54*, 905−921.
22. McRee, D. E. (1999) *J. Struct. Biol. 125*, 156−165.
23. Jefcoate, C. R. (1978) *Methods Enzymol. 52*, 258−279.
24. Mancy, A., Broto, P., Dijols, S., Dansette, P. M., and Mansuy, D. (1995) *Biochemistry 34*, 10365−10375.
25. Daly, J. W., Jerina, D. M., and Witkop, B. (1972) *Experientia 28*, 1129−1264.
26. Guengerich, F. P. (2003) *Arch. Biochem. Biophys. 409*, 59−71.
27. Melet, A., Assrir, N., Jean, P., Pilar Lopez-Garcia, M., Marques-Soares, C., Jaouen, M., Dansette, P. M., Sari, M. A., and Mansuy, D. (2003) *Arch. Biochem. Biophys. 409*, 80−91.
28. Haining, R. L., Jones, J. P., Henne, K. R., Fisher, M. B., Koop, D. R., Trager, W. F., and Rettie, A. E. (1999) *Biochemistry 38*, 3285−3292.

29. Ridderstrom, M., Masimirembwa, C., Trump-Kallmeyer, S., Ahlefelt, M., Otter, C., and Andersson, T. B. (2000) *Biochem. Biophys. Res. Commun. 270*, 983−987.
30. Ellis, S. W., Hayhurst, G. P., Smith, G., Lightfoot, T., Wong, M. M. S., Simula, A. P., Ackland, M. J., Sternberg, M. J. E., Lennard, M. S., Tucker, G. T., and Wolf, C. R. (1995) *J. Biol. Chem. 270*, 29055−29058.
31. Mackman, R., Tschirret-Guth, R. A., Smith, G., Hayhurst, G. P., Ellis, S. W., Lennard, R. S., Tucker, G. T., Wolf, C. R., and De Montellano, P. R. O. (1996) *Arch. Biochem. Biophys. 331*, 134−140.
32. Flanagan, J. U., McLaughlin, L. A., Paine, M. J., Sutcliffe, M. J., Roberts, G. C., and Wolf, C. R. (2002) *Biochem. J.*
33. Paine, M. J., McLaughlin, L. A., Flanagan, J. U., Kemp, C. A., Sutcliffe, M. J., Roberts, G. C., and Wolf, C. R. (2003) *J. Biol. Chem. 278*, 4021−4027.
34. Guengerich, F. P., Miller, G. P., Hanna, I. H., Martin, M. V., Leger, S., Black, C., Chauret, N., Silva, J. M., Trimble, L. A., Yergey, J. A., and Nicoll-Griffith, D. A. (2002) *Biochemistry 41*, 11025−11034.
35. Tsao, C. C., Wester, M. R., Ghanayem, B., Coulter, S. J., Chanas, B., Johnson, E. F., and Goldstein, J. A. (2001) *Biochemistry 40*, 1937−1944.
36. Jung, F., Griffin, K. J., Song, W., Richardson, T. H., Yang, M., and Johnson, E. F. (1998) *Biochemistry 37*, 16270−16279.
37. Klose, T. S., Ibeanu, G. C., Ghanayem, B. I., Pedersen, L. G., Li, L., Hall, S. D., and Goldstein, J. A. (1998) *Arch. Biochem. Biophys. 357*, 240−248.
38. Zerbe, K., Pylypenko, O., Vitali, F., Zhang, W., Rouset, S., Heck, M., Vrijbloed, J. W., Bischoff, D., Bister, B., Sussmuth, R. D., Pelzer, S., Wohlleben, W., Robinson, J. A., and Schlichting, I. (2002) *J. Biol. Chem. 277*, 47476−47485.
39. Podust, L. M., Kim, Y., Arase, M., Neely, B. A., Beck, B. J., Bach, H., Sherman, D. H., Lamb, D. C., Kelly, S. L., and Waterman, M. R. (2003) *J. Biol. Chem. 278*, 12214−12221.
40. Ravichandran, K. G., Boddupalli, S. S., Hasemann, C. A., Peterson, J. A., and Deisenhofer, J. (1993) *Science 261*, 731−736.
41. Haines, D. C., Tomchick, D. R., Machius, M., and Peterson, J. A. (2001) *Biochemistry 40*, 13456−13465.
42. Li, H. Y., and Poulos, T. L. (1997) *Nat. Struct. Biol. 4*, 140−146.
43. Yano, J. K., Koo, L. S., Schuller, D. J., Li, H., Ortiz de Montellano, P. R., and Poulos, T. L. (2000) *J. Biol. Chem. 275*, 31086−31092.
44. Park, S. Y., Yamane, K., Adachi, S., Shiro, Y., Weiss, K. E., and Sligar, S. G. (2000) *Acta Crystallogr. D56*, 1173−1175.
45. Schlichting, I., Berendzen, J., Chu, K., Stock, A. M., Maves, S. A., Benson, D. E., Sweet, R. M., Ringe, D., Petsko, G. A., and Sligar, S. G. (2000) *Science 287*, 1615−1622.

BI034556L